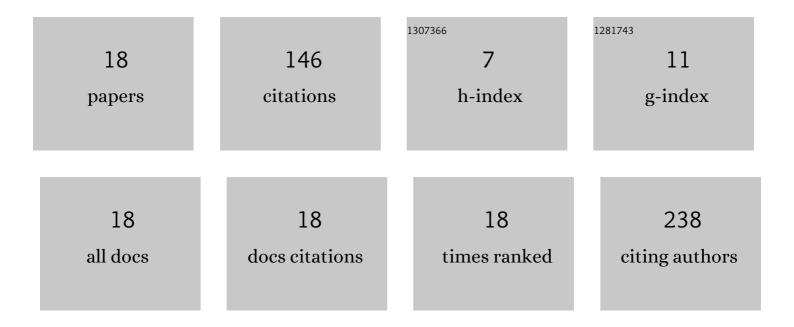
## Toshihiro Furuta

List of Publications by Year in descending order

Source: https://exaly.com/author-pdf/7193433/publications.pdf Version: 2024-02-01



Τοςμιμιρο Ειιριιτλ

#	Article	IF	CITATIONS
1	Full and hybrid iterative reconstruction to reduce artifacts in abdominal CT for patients scanned without arm elevation. Acta Radiologica, 2017, 58, 1085-1093.	0.5	22
2	Recognizing Radiation-induced Changes in the Central Nervous System: Where to Look and What to Look For. Radiographics, 2021, 41, 224-248.	1.4	21
3	Single-energy metal artifact reduction technique for reducing metallic coil artifacts on post-interventional cerebral CT and CT angiography. Neuroradiology, 2018, 60, 1141-1150.	1.1	14
4	Hepatic Segments and Vasculature: Projecting CT Anatomy onto Angiograms. Radiographics, 2009, 29, e37.	1.4	12
5	Multiple-animal MR Imaging using a 3T Clinical Scanner and Multi-channel Coil for Volumetric Analysis in a Mouse Tumor Model. Magnetic Resonance in Medical Sciences, 2011, 10, 229-237.	1.1	10
6	Magnetic resonance microscopy imaging of posterior interosseous nerve palsy. Japanese Journal of Radiology, 2009, 27, 41-44.	1.0	8
7	Artifact-reduced simultaneous MRI of multiple rats with liver cancer using PROPELLER. Journal of Magnetic Resonance Imaging, 2013, 38, 225-230.	1.9	8
8	Hemosuccus Pancreaticus in a Patient with Iodine Allergy: Successful Diagnosis with Magnetic Resonance Imaging and Treatment with Transarterial Embolization Using Carbon Dioxide as the Contrast Medium. CardioVascular and Interventional Radiology, 2009, 32, 1296-1299.	0.9	7
9	Erdheim–Chester disease with an 18F-fluorodeoxyglucose-avid breast mass and BRAF V600E mutation. Japanese Journal of Radiology, 2014, 32, 282-287.	1.0	7
10	Detection of Lung Tumors in Mice Using a 1-Tesla Compact Magnetic Resonance Imaging System. PLoS ONE, 2014, 9, e94945.	1.1	7
11	Magnetic Resonance-Based Visualization of Thermal Ablative Margins Around Hepatic Tumors by Means of Systemic Ferucarbotran Administration Before Radiofrequency Ablation. Investigative Radiology, 2015, 50, 376-383.	3.5	6
12	Delayed hepatic signal recovery on ferucarbotran-enhanced magnetic resonance images: an experimental study in rat livers with gadolinium chloride-induced Kupffer cell damage. Magnetic Resonance Materials in Physics, Biology, and Medicine, 2013, 26, 313-324.	1.1	5
13	Central High Signal in Inflammatory Swollen Lymph Nodes on SPIO-enhanced Interstitial MR Lymphograms: A Mimic of Lymph Node Metastasis. Magnetic Resonance in Medical Sciences, 2012, 11, 61-63.	1.1	4
14	Delayed hepatic signal recovery on ferucarbotran-enhanced magnetic resonance images in a rat model with regional liver irradiation. Magnetic Resonance Materials in Physics, Biology, and Medicine, 2014, 27, 501-508.	1.1	4
15	Intensity Correction Method Customized for Multi-animal Abdominal MR Imaging with 3T Clinical Scanner and Multi-Array Coil. Magnetic Resonance in Medical Sciences, 2013, 12, 95-103.	1.1	4
16	Persistent T2*-hypointensity of the liver parenchyma after irradiation to the SPIO-accumulated liver: An imaging marker for responses to radiotherapy in hepatic malignancies. Journal of Magnetic Resonance Imaging, 2017, 45, 303-312.	1.9	3
17	Fat-forming solitary fibrous tumor of the sacrum: A case report and literature review. Radiology Case Reports, 2021, 16, 1874-1877.	0.2	3
18	Treatment margins in radiotherapy for liver tumors visualized as T2*-hypointense areas on SPIO-enhanced MRI at 9.4ÂT. Magnetic Resonance Materials in Physics, Biology, and Medicine, 2020, 33, 701-712.	1.1	1